Title

Design and Synthesis of Core–Shell Carbon Polymer Dots with Highly Stable Fluorescence in Polymeric Materials

Journal

ACS Applied Nano Materials, 2(10)

ISSN

2574-0970

Authors

Yu, Yuan
Tang, Peixin
Barnych, Bogdan
et al.

Publication Date

2019-10-25

DOI

10.1021/acsanm.9b01446

Peer reviewed

Published in final edited form as:

ACS Appl Nano Mater. 2019 October 25; 2(10): 6503–6512. doi:10.1021/acsanm.9b01446.

Design and Synthesis of Core-Shell Carbon Polymer Dots with Highly Stable Fluorescence in Polymeric Materials

Yuan Yu[†,‡], **Peixin Tang**[‡], **Bogdan Barnych**[§], **Cunyi Zhao**[‡], **Gang Sun**[‡,*], **Mingqiao Ge**[*,†]

[†]College of Textile & Clothing, Jiangnan University, Wuxi 214122, China

[‡]Department of Biological and Agricultural Engineering, University of California, Davis, California 95616, United State

[§]Department of Entomology and Nematology and UCD Comprehensive Cancer Center, University of California, Davis, California 95616, United States

Abstract

In recent years, fluorescent carbon dots have attracted great attention due to their good luminescence and low toxicity. Here, blue fluorescent core-shell structured carbon polymer dots (CPDs) with high stability under a wide range of pH values, long storage time and excellent fluorescence in various solvents and even in solid state were prepared by hydrothermal synthesis of dendritic tris(2-aminoethyl)amine (TAEA) and citric acid. The CPDs core structure provides strong fluorescent luminescence, a shell structure of the core possesses high amount of dendritic primary amino groups connected by ethylene groups to the core. This unique structure prevents aggregation of the cores and self-quenching effect of CPDs. As a result, the CPDs have high fluorescence in both aqueous and hydrophobic solutions and even as pure solid-state powder. In addition, the CPDs are also insensitive to pH of solutions, and the fluorescence intensity of the solution was stable in the pH range of 4–14. The CPDs embedded polymer films and fibers revealed excellent fluorescent properties.

Graphical Abstract

[*]**Corresponding Author:** ge_mingqiao@126.com (M.G.), Tel.: +86-139-1526-9201; gysun@ucdavis.edu (G.S.); Tel.: +1 530-752-0840.

Supporting Information

Synthetic strategy of fluorescent CPDs, a calibration curve of standard TAEA concentrations versus colour intensity, pH values change of CPDs solutions, fluorescence intensities of CPDs in different solvents, fluorescence characterizations of CPDs blend with different polymers (PDF)

The authors declare no competing financial interest.

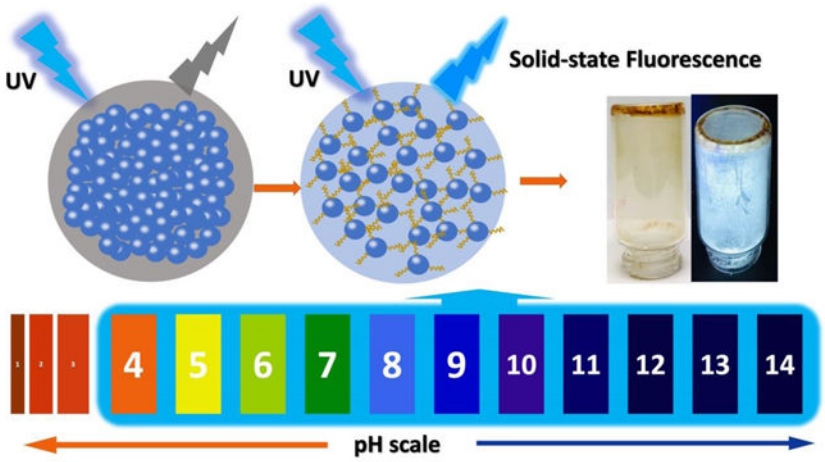

Keywords

carbon polymer dots; solid-state fluorescence; core-shell; dendritic structure; fluorescent polymers

INTRODUCTION

Fluorescent carbon polymer dots (CPDs) are attracting increasing attention due to their bright luminescence, chemical inertness, low cytotoxicity and great biocompatibility[1–4] Many processes for preparing CPDs have been developed, including top-down methods of electrochemical synthesis[5], acidic oxidation[6], ultrasonic synthesis[1], arc discharge[7] and laser ablation[8] and bottom-up methods of carbonization of carbon compounds[9], organic synthesis of small molecules[10], self-assembly of polycyclic aromatic hydrocarbons[11], as well as carbonization and dehydration methods by using hydrothermal[12], microwave[13], and concentrated acid pyrolysis processes[14]. Among these processes, the hydrothermal method has the advantages of being simple, low-cost, and use of natural glucose[15], amino acid[16], citric acid[17], and oligomeric cellulose[18] as start materials. Citric acid is an important precursor material due to its environmental-friendliness, low cost, and ability to directly form CPDs possessing high fluorescence quantum yield (QY)[19, 20]. Doping of citric acid produced CPDs with heteroatoms such as phosphorus, nitrogen, and sulfur could further increase the fluorescence intensity and QY, while nitrogen doping is a simple and effective method to improve fluorescence stability and intensity[21]. To date, a variety of different nitrogen sources have been successfully applied to the fluorescence enhancement of citric acid based CPDs, such as urea, ammonium hydroxide[22], and ethylenediamine (EDA)[23]. Although nitrogen doping has been proven effective in increasing the fluorescence intensity and stability of fluorescent carbon dots, the carbon dots produced are relatively sensitive to pH and not adapting to a wide range of pH changes[22], and become self-quenched in solid state[23]. Therefore, it is still a challenging and important issue to develop CPDs with improved stability in a wide pH range and long shelf lifetime and applicable in various solvents and polymeric materials.

The carbon dots prepared from urea and ammonia as nitrogen sources showed self-quenching phenomenon in the solid state due to potential resonance energy transfer (RET)

or π-π interactions[24–26] of fluorophores. Thus, prevention of aggregation and dispersion of the nitrogen doped CPDs in solid materials such as polymers[27], starch[28] and silica xerogel[29] are key factors in preparation of solid-state fluorescent materials. Therefore, we designed a new type of carbon dots possessing core-shell structural features with the core serving as a photoluminescence center and the shell serving as a protective layer preventing formation of aggregated photo-active cores and penetration of other elements affecting the cores (Figure 1). Such a structure should provide CPDs with high fluorescent efficiency and stability in various solvents and polymers.

In this study, the new citric acid based core-shell structured CPDs were prepared by following a simple hydrothermal one-pot method using tris(2-aminoethyl)amine (TAEA) as a nitrogen source. TAEA is a compound capable of forming dendritic structure due to existence of abundant amino groups, which has never been applied in the preparation of CPDs previously. The TAEA not only can serve as a nitrogen source in the formation of fluorescent CPDs but also could form a layer of abundant primary amino groups isolated from the core by ethylene units (Figure 1). Compared with traditional CPDs prepared from urea and ammonia, the new CPDs showed strong fluorescence not only in aqueous solutions but also in a pure solid-state material. After the prepared CPDs solution was stored for 2 months at room temperature, it still exhibited strong fluorescence. And in the pH range of 4–14, the fluorescence of the CPD solution was stable, showing an excellent stability of the CPDs in a wide range of pH values. Polymer films and fibers containing the CPDs also exhibited excellent fluorescent properties.

RESULTS AND DISCUSSION

Synthesis of core-shell CPDs

A synthesis scheme of the CPDs is shown in Figure S1 and briefed in Figure 1. TAEA can act as a surface passivation agent on the CPDs and also can participate in the formation of the CPDs core with a shell structure due to the existence of multiple primary amino groups. The amino groups in TAEA are separated from a central tertiary nitrogen atom by ethylene groups, isolating the fluorescent core CPDs from a spherical layer of the primary amino groups and preventing any potential n-π conjugation from nitrogen atoms to the core. Therefore, the fluorescence quenching of the CPDs induced by electron transitions will be blocked by the ethylene groups. Finally, the novel CPDs with the structural features and desired properties were prepared, and a high QY (64.5 %) was achieved successfully in aqueous solutions. The CPDs showed bright fluorescence in an aqueous solution, as shown in Figure 1.

Optimization of preparation conditions

After confirmation of the basic CPDs structures and the desired fluorescence, reaction times, temperatures and concentration ratios of reagents were varied to optimize the formation of the CPDs. The absorption and emission spectra of the CPD solutions synthesized under different reaction durations (from 2 h to 24 h) are shown in Figure 2a. The absorption and emission spectra revealed a similar trend in both intensities. The fluorescence intensity increased significantly as the reaction time prolonged from 2 h to 6 h and reached a

maximum at 6 h, indicating completion of the formation of the core-shell CPDs. Prolonged reaction time may cause damage to the formed ethylene-primary amine shell due to potential degradation of the groups under high temperature. Thus, the fluorescence intensity decreased slightly as the reaction time further increased. The hydrothermal reaction requires high temperature, but very high temperature will cause the degradation of the formed CPDs, especially the ethylene amino groups on the shell. The loss of the dendritic shell on the CPDs will lead to nanoparticle aggregations and quenching, and consequently resulting in reduced fluorescence. So, the UV-vis absorption and fluorescence of the samples synthesized under different temperatures with a reaction time of 6 h varied accordingly (Figure 2b). When the reaction temperature was increased from 120 °C to 160 °C, both the absorption and emission of the samples increased gradually, except the adsorption at 160 °C, which could be a critical point of potential degradation of the shell structures. Temperatures higher than 160 °C definitely damaged the core-shell CPD structure and lowered the fluorescence intensity.

The absorption and emission spectra of the CPDs prepared by using different molar ratios of citric acid and TAEA were studied (Figure 2c). The results revealed that when the molar ratio of citric acid: TAEA was 1:0.1, the fluorescence intensity of the CPDs was extremely low, indicating the importance of the nitrogen compound in providing the photoactive effect. When the molar ratios were increased to 1:0.5 and then 1:0.7, the fluorescence intensities were increased and reached the maximum. An equal amount of citric acid and TAEA is expected to produce a neutral product. The pH values of the CPD aqueous solutions prepared with different molar ratios of citric acid/ TAEA were measured, and the results are shown in Figure S2. At the molar ratio of citric acid /TAEA of 1:0.5, the CPDs solution was neutral. Increased TAEA contents in the CPDS increased pH values of aqueous solutions, but the pH values of the solutions weres stabilized at slightly above 8. These results supported the structural feature of the core-shell CPDs (Figure 1), indicating that TAEA not only passivated the core CPDs but also participated in the formation of a shell on the CPDs.

Characterization of core-shell CPDs

The CPDs cores are mainly composed of carbon condensed from citric acid with amide structures formed due to nitrogen doping effect of TAEA[8, 30]. The CPDs revealed strong absorption in both UVC and UVA regions in the UV-vis absorption spectrum (Figure 3a) with two peaks at 250 nm and 350 nm in aqueous solution. A strong fluorescence emission peak was centred at around 445 nm, as shown in Figure 3b. The emission spectra indicated that the CPDs possess excitation-wavelength-dependent photoluminescence (PL)[31, 32]. When the excitation wavelength was changed from 240 nm to 360 nm, the emission peak remained at 445 nm. With the excitation wavelength further increased, the emission intensity significantly decreased and the peak shifted to longer wavelengths. Although a detailed mechanism of excitation-wavelength-dependent PL of the CPDs remains unanswered, the emission characteristics of the CPDs under longer excitation wavelength could be attributed to reduced absorption and excitation and varied emissive sites located on the surface of CPDs[33]. The unique fluorescence properties of the CPDs offer an additional advantage in distinguishing excitation wavelengths according to the different emissions, which could be applied in fluorescent sensors, anti-counterfeit labels and fluorescence imaging.

Drops of the CPDs aqueous solution were deposited on a carbon-coated copper grid for TEM analysis. The particle size and morphology of the CPDs were observed. The particles were distributed evenly on the copper grid, demonstrating excellent dispersion of the CPDs in the solutions. The particle size and distribution of CPDs were analyzed by a statistical software[34], with results showing that the CPDs were narrowly-distributed nanoparticles and the average diameter was 3 nm (Figure 3c). As shown in the TEM image, the CPDs possess a clear two-dimensional lattice structure. The spacing is 0.21 nm by accurate measurement, similar to the lattice spacing of graphite 2H of graphitic (sp^2) carbon[35]. The XRD pattern displays a broad diffraction peak due to the small size of CPDs, indicating the nanocrystalline characteristics of the sample[36] (Figure 3d). The diffraction peaks in the XRD pattern are basically same as those of graphite 2H according to the Powder Diffraction File (PDF) card[36], which are in good agreement with the results of the TEM images.

The X-ray photoelectron spectroscopy (XPS) spectrum of the CPDs (Figure 4a) shows three peaks at 284.7, 399.7 and 530 eV, attributing to C1s, N1s, and O1s, respectively. In addition, the CPDs contains 67.6 at. *%* of C element, 15.6 at. *%* of O element, and 16.8 at. % of N element according to the corresponding binding energies in Figure 4a. The C1s spectrum (Figure 4b) can be deconvoluted to four peaks at 283.9, 284.9 and 287.2 eV, corresponding to C-N, C-C/C=C, and C=N/C=O, respectively[37, 38]. The N1s spectrum (Figure 4c) has three peaks at 398.3, 399.4 and 400.9 eV, attributing to C-N-C, N-(C)3 and N-H, respectively. The structural features measured by XPS illustrate the participation of N atoms in the synthesis reaction of the CPDs[39]. The functional groups of the CPDs were detected by FT-IR (Figure 4d). The broad absorption band at 3200–3550 cm^{-1} is ascribed to –OH and $–NH_2$ bonds. The appearance of 2950 cm^{-1} and 2844 cm^{-1} are attributed to the C-H bond. The bands at 1780 cm^{-1} and 1710 cm^{-1} are attributed to C=O of COOH. The absorptions at 1655 cm^{-1} and 1570 cm^{-1} prove the existence of amide I, amide II, respectively, further confirming the existence of amide structure in the CPDs[40, 41].

Due to the structural feature of TAEA, excess amount of primary amino groups should exist on the surfaces of the CPDs. The quantity of total primary amino groups on the surface of CPDs was determined by following a traditional ninhydrin colorimetry method. Ninhydrin could react with primary amino group and produce a compound with a deep purple colour known as Ruhemann’s purple, as shown in Figure S2. The intensities of absorption at 569 nm are positively proportional to the concentration of the amino groups in a certain range. A calibration curve was prepared by using standardized TAEA concentrations, showed in Figure S2a. The primary amino groups on the surface of the core-shell CPDs were compared with that of the CPDs prepared from urea with the same concentration. It was found the core-shell CPDs contain about 3.2 times more primary amino groups than the ones made from using urea as a nitrogen source, confirming the abundant amino groups on the surface of the CPDs prepared from the TAEA.

Stability under different conditions

The stability of fluorescence intensity is crucial in the practical application of CPDs, which could be affected by different nitrogen sources employed in the synthesis[42]. The core-shell structured CPDs prepared from TAEA should possess outstanding stability for long-term

storage, especially compared to ammonium hydroxide and urea based CPDs prepared under the same conditions. The fluorescence intensities of these samples in aqueous solutions were measured after one- and two-months storage under the same condition for one and two months, respectively. The results revealed that after storage in the air for one month, the fluorescence intensities of three samples were reduced to 63%, 71% and 90% of the original samples prepared from ammonium hydroxide, urea and TAEA as nitrogen sources, respectively. The intensities of the samples further reduced to 43%, 57% and 78% of the original samples after two months of storage (Figure 5a–c). Obviously, the sample prepared by using TAEA as a nitrogen source proved to have the best stability. The core-shell CPDs possessed excess amount of dendritic amino groups on the shell surface, preventing aggregations of the CPDs in solvents and even in solid state (Figure 5d). Such a result further supports the structural features of the CPDs confirmed by chemical analysis.

The ethylene connection units between the fluorescent CPDs core and rich amino shell prevent potential electron transitions internally and ensure good fluorescence at condensed phases such as solid or in different polymer media. As shown in Figure 6a, the core-shell CPDs (CPDs 1) displayed the strongest fluorescence intensity in a solid-state form, while the CPDs prepared from citric acid and urea (CPDs 4) or ammonia (CPDs 5) did not show any fluorescence in solid-states (Figure 6b). The unique shell surface of the CPDs provided by TAEA effectively prevents the aggregation of these nanoparticles, as shown in Figure 6c. To further confirm the contribution of TAEA serving as a shell on a fluorescent core, we prepared different CPDs by using aconitic acid (CPDs 2) and tricarboxylic acid (CPDs 3) as different carbon sources, respectively, with TAEA as the nitrogen source. Both products (CPDs 2 and CPDs 3) also revealed fluorescence in solid powder forms, with the intensities still strong but slightly weaker than that of the CPDs prepared from citric acid (Figure 6a and Figure 6b). Those results all served as evidence of formation and protective function of the dendritic amino shell from TAEA on the fluorescent cores of the CPDs.

The CPDs prepared from TAEA (CPDs 1) and urea (CPDs 4) were dissolved in different solvents and then tested the fluorescence intensities, respectively (Figure S4). The results showed the fluorescence intensities of both CPDs decreased with the reduction of the solvent polarity. However, in the very hydrophobic solvent, hexane, the CPDs 1 still retained similar fluorescent intensity to the solid powder. The CPDs 4 were totally quenched in hexane solvents and also in solid powder form. This result again proved the core-shell CPDs' unique properties.

The dendritic amino groups on the shell of the CPDs could interact with excess amount of protons in aqueous solution and protect the fluorescent core intact in a wide range of pH values. This structural feature could significantly improve fluorescence stability of the CPDs under different pH conditions, which has been an interest to many researchers[31, 43, 44] The fluorescence intensities of the core-shell CPDs were tested in a range of pH 1–14 in aqueous solutions (Figure 7a), and the fluorescence intensities were very stable for 60 hours under continuous exposure to 365 nm UV light at room temperature (Figure 7b). The fluorescence intensity of the CPDs solutions were almost unchanged in a pH range of 4–14, but decreased rapidly as the pH was reduced from 4 to 1. Excess amount of primary amino groups on the shell could be protonated by high concentrations of H^+ to form cationic $–N^+H3$ groups

which are more repulsive to protons, preventing penetration of the H^+ into the fluorescent cores (Figure 7c). The fluorescence intensities of the solutions were nearly constant in the pH range of 4–14, which was better than the reported results of the other CPDs prepared from using different nitrogen sources[45]. Overall, alkaline and weaker acidic conditions would not be able to break through the protective shell layer and affect the carbon core of the CPDs (Figure 7c), making the CPDs applicable in the pH of 4–14[46, 47] However, the fluorescence intensity decreased when pH of solutions was further lowered and became extremely acidic (<4), the proton concentration was increased to a level that the ions can penetrate through the protective shell due to a high potential created by the concentration difference and attack the CPDs core[48]. This quenching reaction was reversible if the solution was re-adjusted back to pH above 4 and the fluorescence intensity kept stable after 6 cycles, as shown in Figure 7d.

Application in Polymeric Materials

The prepared core-shell CPDs demonstrated high fluorescence in both hydrophobic and hydrophilic solvents and also in solid state, revealing possibility for producing fluorescent polymers if properly embedded. As an example, a hydrophobic fiber-forming polymer, polyacrylonitrile (PAN) was mixed with the hydrophilic core-shell CPDs in solutions and then spun into fluorescent PAN fibers. The fluorescent PAN fibers are coded as FPAN-1, FPAN-2, FPAN-3, FPAN-4, and FPAN-5, representing the CPD concentrations in the PAN fibers as 0.01 wt.%, 0.05 wt.%, 0. 2 wt.%, 0.5 wt.% and 1.0 wt.%, correspondingly. The fluorescent excitation and emission of the FPANs were tested, and the result showed that the FPANs possess the same excitation and emission wavelengths with the CPDs. The emission intensity increased with the increasing concentration of the CPDs in the PAN matrix and then keep stable when the concentration was 1.0 wt.%. This result indicated the hydrophilic CPDs could mix well with the hydrophobic polymer and produce the fluorescent fibers, which is another solid evidence of the designed core-shell CPDs structure and excellent performance. The fluorescent characterizations of the PAN fibers under the illumination of both visible and UV light are shown in Figure S5.

The core-shell CPDs were also blended with different hydrophilic polymers, including cellulose, poly(vinyl alcohol-co-ethylene) (PVA-co-PE), and agarose, as well as PAN, and the blends were casted into films. The films all demonstrated good and durable fluorescence. As shown in Figure S6, the strong fluorescence on the films were stable after stored in the air at room temperature for more than 2 months, indicating that the CPDs possess excellent compatibility and good stability in different polymers.

CONCLUSIONS

In summary, amino rich and dendritic core-shell structured CPDs were prepared by a simple hydrothermal method using citric acid as a carbon source and TAEA as a nitrogen source. The dendritic structure and excess free amino groups on the surface of the CPDs act as “protective shell”, which have a huge repulsive force to prevent the aggregation of these nanoparticles, making these CPDs with strongly fluorescent in various solvents and even as solid-state powder. The prepared CPDs have wide pH tolerance and a relatively stable

fluorescence intensity in the pH range of 4 to 14. The storage stability of the CPDs is excellent, with 78% of original intensity retained after two months of storage. The CPDs can be mixed with both hydrophilic and hydrophobic polymers and produce strong fluorescent fibers and films.

EXPERIMENTAL SECTION

Preparation of CPDs

All chemicals were purchased from vendors of either Acros or Aldrich and used as received. The core-shell CPDs were synthesized by a hydrothermal method using citric acid as a carbon source and TAEA as a nitrogen source at an appropriate temperature for several hours. When the reaction kettle was returned to room temperature, the sample was taken out and dialyzed for 48 hours with a dialysis bag having a molecular weight of 3000, during which time the water was continuously changed. The contents of the dialysis bag were collected and subjected to rotary evaporation and freeze drying. A brown powder was finally obtained and used in subsequent tests and application.

CPDs 2 and CPDs 3 were prepared from aconitic acid and tricarboxylic acid as carbon sources, respectively, TAEA as a nitrogen source, and the molar ratio was 2:1. CPDs 4 was prepared from using citric acid and urea, and the molar ratio was 2:1.5. CPDs 5 was prepared from citric acid and ammonia, and the molar ratio was 2:3. All the CPDs were prepared at 160 °C for 4h by the hydrothermal method, the solid powders were collected following the same procedure as the core-shell CPDs (CPDs 1).

Preparation of Fluorescent PAN Fibers

DMSO was applied as a solvent to dissolve PAN powder, the ratio of PAN and DMSO is 20% (w/v). A concentrated CPD DMSO solution was prepared. Different concentrations of CPDs in the PAN matrix solutions were prepared, and then stirred until the spinning solution become transparent. The fibers were prepared by a wet spinning method with water applied as a coagulation bath. The spinning solution was extruded into water and formed into fibers immediately. The needle was 23G, and the pumping speed was 6 mL/min.

Characterization

X-ray diffraction (D8 Advance X-ray diffractometer, Bruker AXS, Germany) was used to measure the phase composition of the CPDs powder by a Cu Kα radiation at a voltage of 40 kV and current of 40mA under a scan speed of 0.1sec/step at room temperature. The diffraction angle 2θ ranges from 10° to 70°. X-ray photoelectron spectrometry (XPS) experiments were performed by a Thermal ESCALAB 250XI X-ray source system (Thermo Fisher Scientific, USA). The excitation and emission spectra of the CPDs aqueous solutions were recorded on a spectrofluorometer (FS5, Edinburgh Instruments, England) at room temperature. The absolute quantum yield (QY) of this CPDs was measured by the spectrofluorometer (FS5, Edinburgh Instruments, England) at room temperature. The UV-vis absorption spectra of CPDs aqueous solutions were recorded by an UV-mini1240 spectrophotometer (Shimadzu, Japan). Fourier transform infrared (FT-IR) spectroscopy was conducted on a Bruker IFS 66/S spectrophotometer. The pure CPDs powder was mixed with

KBr and then compressed into a crucible for FTIR scanning. The spectra were recorded over the range 4000–500cm^{-1} with a resolution of 4 cm^{-1}. Morphology of the samples were analyzed by a high-resolution transmission electron microscopy (TEM) on Hitachi 9500 TEM and Hitachi HD-2000 STEM systems.

Supplementary Material

Refer to Web version on PubMed Central for supplementary material.

ACKNOELEDGMENTS

This work was financially supported by the National High-tech R&D Program of China (No.2016YFB0302901-3), the Fundamental Research Funds for The Central Universities (JUSRP51723B), National Natural Science Funds (NO.11502230), Production, Education & Research Cooperative Fund of Jiangsu Province (No. BY2016065-25), Jiangsu province ordinary university academic degree graduate student scientific research innovation projects (NO. KYLX16_0798), and National Institute of Environmental Health Science Superfund Research Program (P42ES004699). Y. Yu is grateful for a scholarship fund from the China Scholarship Council for studying at the University of California, Davis.

REFERENCES

1. Li H; He X; Liu Y; Huang H; Lian S; Lee ST; Kang Z, One-step ultrasonic. synthesis of water-soluble carbon nanoparticles with excellent photoluminescent properties. Carbon 2011, 49, 605.
2. Ye R; Xiang C; Lin J; Peng Z; Huang K; Yan Z; Cook NP; Samuel EL; Hwang CC; Ruan G, Coal as an abundant source of graphene quantum dots. Nat. commu 2013, 4, 2943.
3. Hu L; Sun Y; Li S; Wang X; Hu K; Wang L; Liang X; Wu Y, Multifunctional carbon dots with high quantum yield for imaging and gene delivery. Carbon 2014, 67, 508
4. Xia C; Tao S; Zhu S; Song Y; Feng T; Zeng Q; Liu J; Yang B, Hydrothermal. Addition Polymerization for Ultrahigh-yield Carbonized Polymer Dots with Room Temperature Phosphorescence via Nanocomposite. Chem. Eur. J, 2018, 24,11303 [PubMed: 29904946]
5. Li M; Hu C; Yu C; Wang S; Zhang P; Qiu J, Organic amine-grafted carbon. quantum dots with tailored surface and enhanced photoluminescence properties. Carbon 2015, 91, 291.
6. Shen J; Zhu Y; Yang X; Li C, Graphene quantum dots: emergent nanolights for. bioimaging, sensors, catalysis and photovoltaic devices. Chem. Commun 2012, 48, 3686.
7. Dey S; Govindaraj A; Biswas K; Rao C, Luminescence properties of boron and nitrogen. doped graphene quantum dots prepared from arc-discharge-generated doped graphene samples. Chem. Phys. Lett 2014, 595, 203.
8. Sun YP; Zhou B; Lin Y; Wang W; Fernando KS; Pathak P; Meziani MJ; Harruff BA; Wang X; Wang H, Quantum-sized carbon dots for bright and colorful photoluminescence. J. Am. Chem. Soc 2006, 128, 7756. [PubMed: 16771487]
9. Yang Z; Xu M; Liu Y; He F; Gao F; Su Y; Wei H; Zhang Y, Nitrogen-doped, carbon-rich, highly photoluminescent carbon dots from ammonium citrate. Nanoscale 2014, 6, 1890. [PubMed: 24362823]
10. Qian Z; Ma J; Shan X; Shao L; Zhou J; Chen J; Feng H, Surface functionalization of graphene quantum dots with small organic molecules from photoluminescence modulation to bioimaging applications: an experimental and theoretical investigation. RSC Adv. 2013, 3, 14571.
11. Liu R; Wu D; Feng X; Mullen K, Bottom-up fabrication of photoluminescent graphene. quantum dots with uniform morphology. J. Am. Chem. Soc 2011, 133, 15221. [PubMed: 21894989]
12. Zhang Z; Hao J; Zhang J; Zhang B; Tang J, Protein as the source for synthesizing. fluorescent carbon dots by a one-pot hydrothermal route. RSC Adv. 2012, 2, 8599.
13. Wang X; Qu K; Xu B; Ren J; Qu X, Microwave assisted one-step green synthesis of. cell-permeable multicolor photoluminescent carbon dots without surface passivation reagents. J. Mater. Chem 2011, 21, 2445.

14. Liu H; Ye T; Mao CJ, Fluorescent carbon nanoparticles derived from candle soot. Angew. Chem. Int. Edit 2007, 46 , 6473.
15. Yang ZC; Wang M; Yong AM; Wong SY; Zhang XH; Tan H; Chang AY; Li X; Wang J, Intrinsically fluorescent carbon dots with tunable emission derived from hydrothermal treatment of glucose in the presence of monopotassium phosphate. Chem. Commun 2011, 47, 11615.
16. Zeng YW; Ma DK; Wang W; Chen JJ; Zhou L; Zheng YZ; Yu K; Huang SM, N, S co-doped carbon dots with orange luminescence synthesized through polymerization and carbonization reaction of amino acids. Appl. Surf. Sci 2015, 342, 136.
17. Dong Y; Shao J; Chen C; Li H; Wang R; Chi Y; Lin X; Chen G, Blue luminescent graphene quantum dots and graphene oxide prepared by tuning the carbonization degree of citric acid. Carbon 2012, 50, 4738.
18. da Silva Souza DR; Caminhas LD; de Mesquita JP; Pereira FV; Physics, Luminescent carbon dots obtained from cellulose. Mater. Chem. Phys 2018, 203, 148.
19. Song Y; Zhu S; Zhang S; Fu Y; Wang L; Zhao X; Yang B, Investigation from. chemical structure to photoluminescent mechanism: a type of carbon dots from the pyrolysis of citric acid and an amine. J.Mater. Chem. C 2015, 3, 5976.
20. Wang F; Kreiter M; He B; Pang S; Liu C, Synthesis of direct white-light emitting. carbogenic quantum dots. Chem. Commun 2010, 46, 3309.
21. Wang ZX; Ding SN, One-pot green synthesis of high quantum yield oxygen-doped, nitrogen-rich, photoluminescent polymer carbon nanoribbons as an effective fluorescent sensing platform for sensitive and selective detection of silver (I) and mercury (II) ions. Anal. Chem 2014, 86, 7436. [PubMed: 24979236]
22. Mao XJ; Zheng HZ; Long YJ; Du J; Hao JY; Wang LL; Zhou DB, Study on the fluorescence characteristics of carbon dots. Spectrochim. Acta. A 2010, 75, 553.
23. Zhou D; Li D; Jing P; Zhai Y; Shen D; Qu S; Rogach A, Conquering aggregation-induced solid-state luminescence quenching of carbon dots through a carbon dots-triggered silica gelation process. Chem. Mater 2017, 29, 1779.
24. Chiang CL; Wu MF; Dai DC; Wen YS; Wang JK; Chen CT, Red-Emitting. Fluorenes as Efficient Emitting Hosts for Non-Doped, Organic Red-Light-Emitting Diodes. Adv. Funct. Mater 2005, 15, 231.
25. Chen Y; Zheng M; Xiao Y; Dong H; Zhang H; Zhuang J; Hu H; Lei B; Liu Y, A self-quenching-resistant carbon-dot powder with tunable solid-state fluorescence and construction of dual-fluorescence morphologies for white light-emission. 2016, 28 (2), 312–318.
26. Li H; Zhang Z; Ding J; Xu Y; Chen G; Liu J; Zhao L; Huang N; He Z; Li Y, Diamond-like carbon structure-doped carbon dots: A new class of self-quenching-resistant solid-state fluorescence materials toward light-emitting diode. Carbon 2019, 149, 342.
27. Li X; Zhang S; Kulinich SA; Liu Y; Zeng H, Engineering surface states of carbon dots. to achieve controllable luminescence for solid-luminescent composites and sensitive Be^{2+} detection. SCI. Rep 2014, 4, 4976.
28. Sun M; Qu S; Hao Z; Ji W; Jing P; Zhang H; Zhang L; Zhao J; Shen D, Towards efficient solid-state photoluminescence based on carbon-nanodots and starch composites. nanoscale 2014, 6, 13076. [PubMed: 25247822]
29. Xie Z; Wang F; Liu CY, Organic-inorganic hybrid functional carbon dot gel glasses. Adv.Mater 2012, 24, 1716. [PubMed: 22396335]
30. Zhu S; Meng Q; Wang L; Zhang J; Song Y; Jin H; Zhang K; Sun H; Wang H; Yang B, Highly photoluminescent carbon dots for multicolor patterning, sensors, and bioimaging. Angew. Chemie 2013, 125, 4045.
31. Jia X; Li J; Wang E, One-pot green synthesis of optically pH-sensitive carbon dots with. upconversion luminescence. Nanoscale 2012, 4, 5572. [PubMed: 22786671]
32. Wang H; Sun C; Chen X; Zhang Y; Colvin VL; Rice Q; Seo J; Feng S; Wang S; William W, Excitation wavelength independent visible color emission of carbon dots. Nanoscale 2017, 9, 1909. [PubMed: 28094404]

33. Zhang YQ; Ma DK; Zhuang Y; Zhang X; Chen W; Hong LL; Yan QX; Yu K; Huang SM, One-pot synthesis of N-doped carbon dots with tunable luminescence properties. J. Mater. Chem 2012, 22, 16714.
34. Gallego-Urrea JA; Tuoriniemi J; Hassellov M, Applications of particle-tracking analysis to. the determination of size distributions and concentrations of nanoparticles in environmental, biological and food samples. TrAC Trends in Anal. Chem 2011, 30, 473.
35. Zhang Z; Cai Z; Peng J; Zhu M, Comparison of the tribology performance of nano-diesel. soot and graphite particles as lubricant additives. J. of Phys. D: Appl. Phys, 2015, 49, 045304.
36. Dong Y; Shao J; Chen C; Li H; Wang R; Chi Y; Lin X; Chen G, Blue luminescent graphene quantum dots and graphene oxide prepared by tuning the carbonization degree of citric acid. Carbon 2012, 50, 4738.
37. Qu S; Liu X; Guo X; Chu M; Zhang L; Shen D, Amplified spontaneous green emission and lasing emission from carbon nanoparticles. Adv. Funct. Mater 2014, 24, 2689.
38. Liao J; Cheng Z; Zhou L; Nitrogen-doping enhanced fluorescent carbon dots: green synthesis and their applications for bioimaging and label-free detection of Au^{3}+ ions. ACS Sustainable Chem. Eng 2016, 4, 3053–3061.
39. Wang L; Ruan F; Lv T; Liu Y; Deng D; Zhao S; Wang H; Xu S, One step synthesis of Al/N co-doped carbon nanoparticles with enhanced photoluminescence. J. Lumin 2015, 158, 1.
40. Mochalin VN; Gogotsi Y, Wet chemistry route to hydrophobic blue fluorescent nanodiamond. J. Am. Chem. Soc 2009, 131, 4594. [PubMed: 19290627]
41. Li M; Hu C; Yu C; Wang S; Zhang P; Qiu J, Organic amine-grafted carbon quantum dots with tailored surface and enhanced photoluminescence properties. Carbon 2015, 91, 291.
42. Qu D; Zheng M; Zhang L; Zhao H; Xie Z; Jing X; Haddad RE; Fan H; Sun Z, Formation mechanism and optimization of highly luminescent N-doped graphene quantum dots. Sci. rep 2014, 4, 5294. [PubMed: 24938871]
43. Xiao Q; Liang Y; Zhu F; Lu S; Huang S, Microwave-assisted one-pot synthesis of highly luminescent N-doped carbon dots for cellular imaging and multi-ion probing. Microchim. Acta 2017, 184, 2429.
44. Hill SA; Benito-Alifonso D; Morgan DJ; Davis SA; Berry M; Galan MC, Three-minute synthesis of sp 3 nanocrystalline carbon dots as non-toxic fluorescent platforms for intracellular delivery. 2016, 8, 18630.
45. Hou Y; Lu Q; Deng J; Li H; Zhang Y, One-pot electrochemical synthesis of functionalized fluorescent carbon dots and their selective sensing for mercury ion. Anal. Chim. Acta 2015, 866, 69. [PubMed: 25732694]
46. Zheng C; An X; Gong J, Novel pH sensitive N-doped carbon dots with both long fluorescence lifetime and high quantum yield. RSC Adv. 2015, 5, 32319.
47. Kong W; Wu H; Ye Z; Li R; Xu T; Zhang B, Optical properties of pH-sensitive carbon-dots with different modifications. J. Lumin 2014, 148, 238.
48. Shi W; Li X; Ma H, A tunable ratiometric pH sensor based on carbon nanodots for the quantitative measurement of the intracellular pH of whole cells. Angew. Chem. Int. Edit 2012, 51, 6432–6435

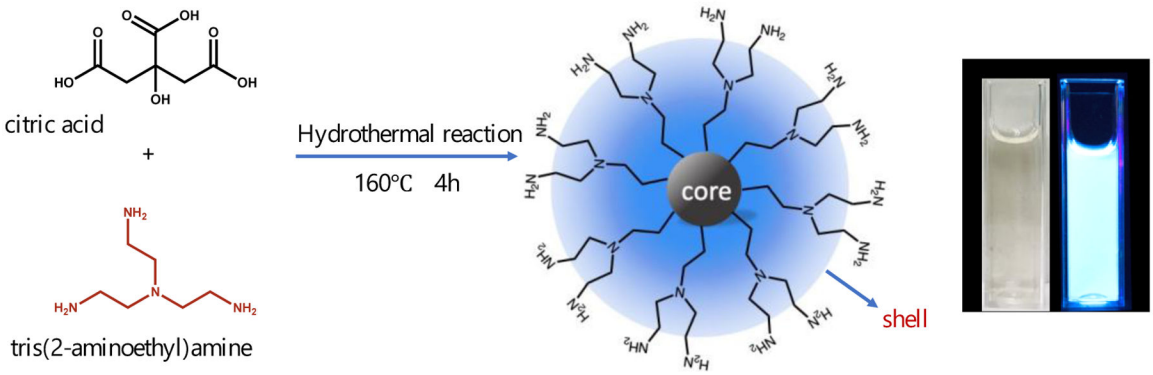

Figure 1.
Schematic illustration of the possible formation process and the surface state of the CPDs

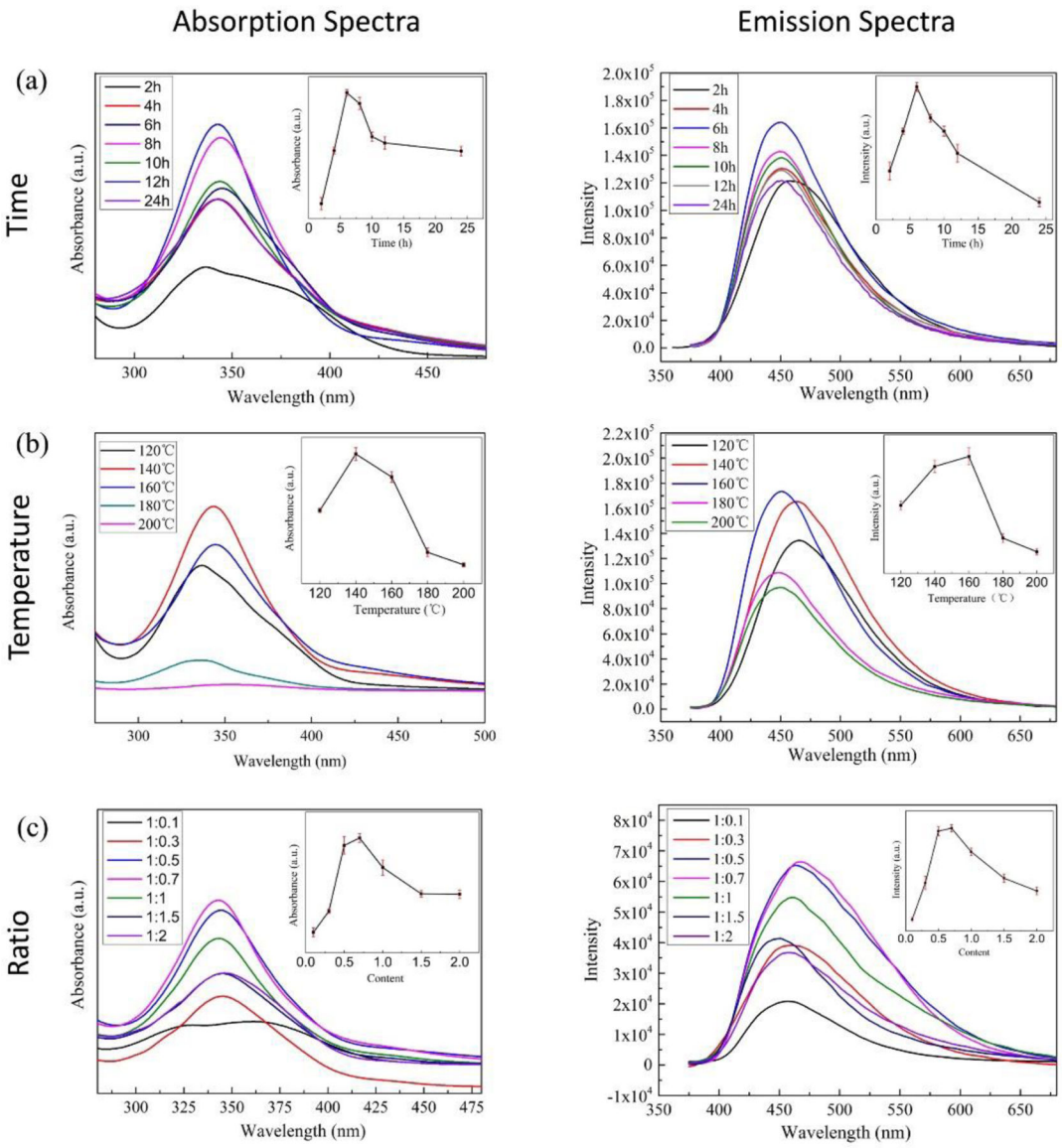

Figure 2.

Spectra of UV-Vis absorption and emission of samples prepared (a) at different reaction times at the temperature of 160 °C, (b) at different reaction temperatures for 6 h and (c) at different molar ratios of raw materials.

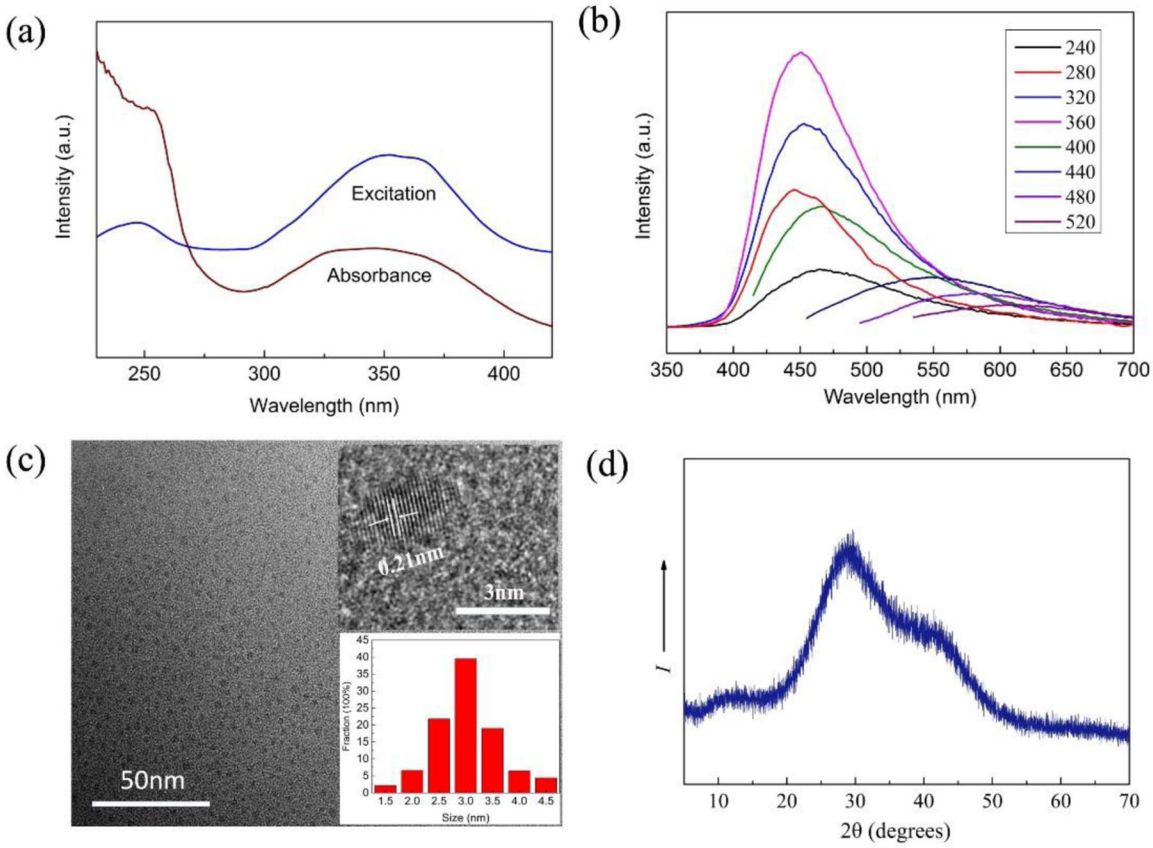

Figure 3.

Optical characterization of CPDs: (a) UV-vis spectrum; (b) emission spectra under excitations of different wavelengths; (c) TEM images of CPDs at low and high magnifications (d) XRD pattern. The inserts in (c) are a representative images of individual CPDs with graphite structure (upper) and the size distribution of CPDs (lower).

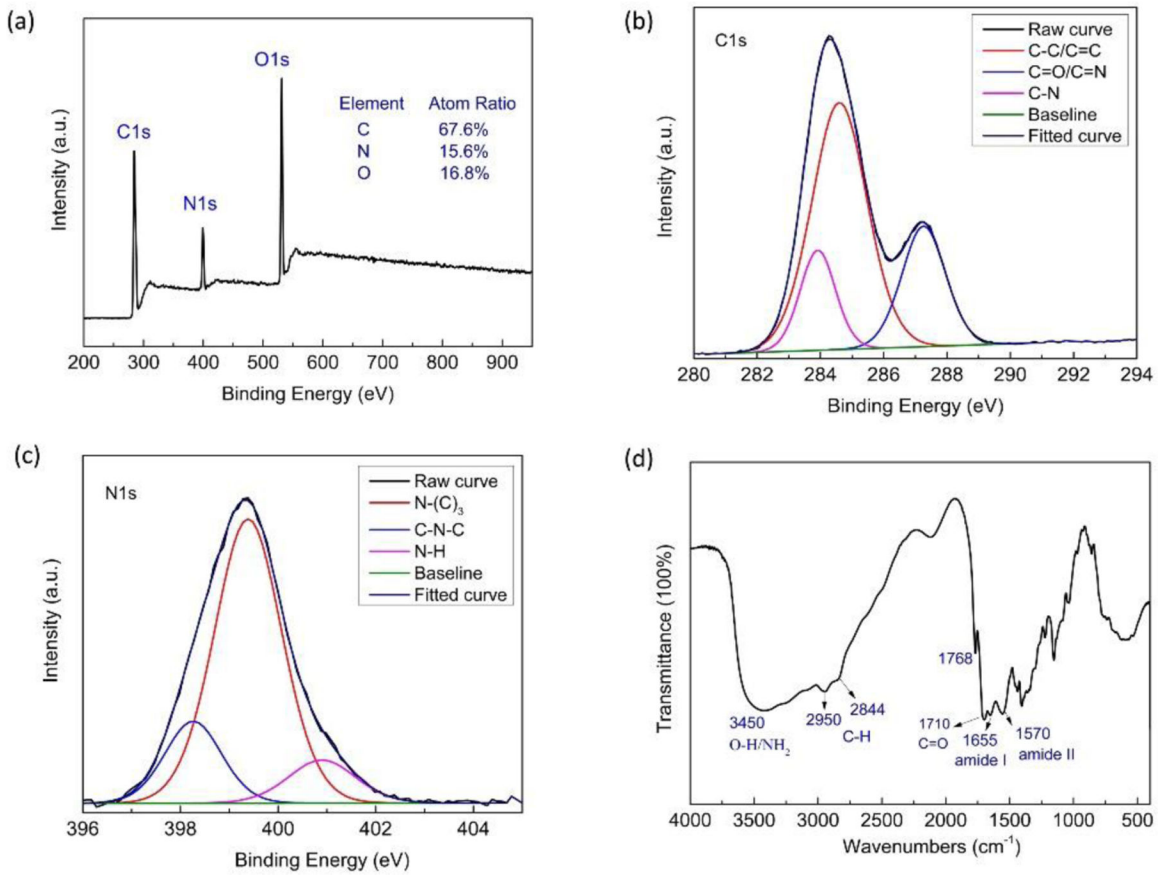

Figure 4.

(a) XPS survey spectrum; (b) the high-resolution C1s peaks and the fitting curves; (c) N1s peaks and the fitting curves; (d) the FT-IR spectrum

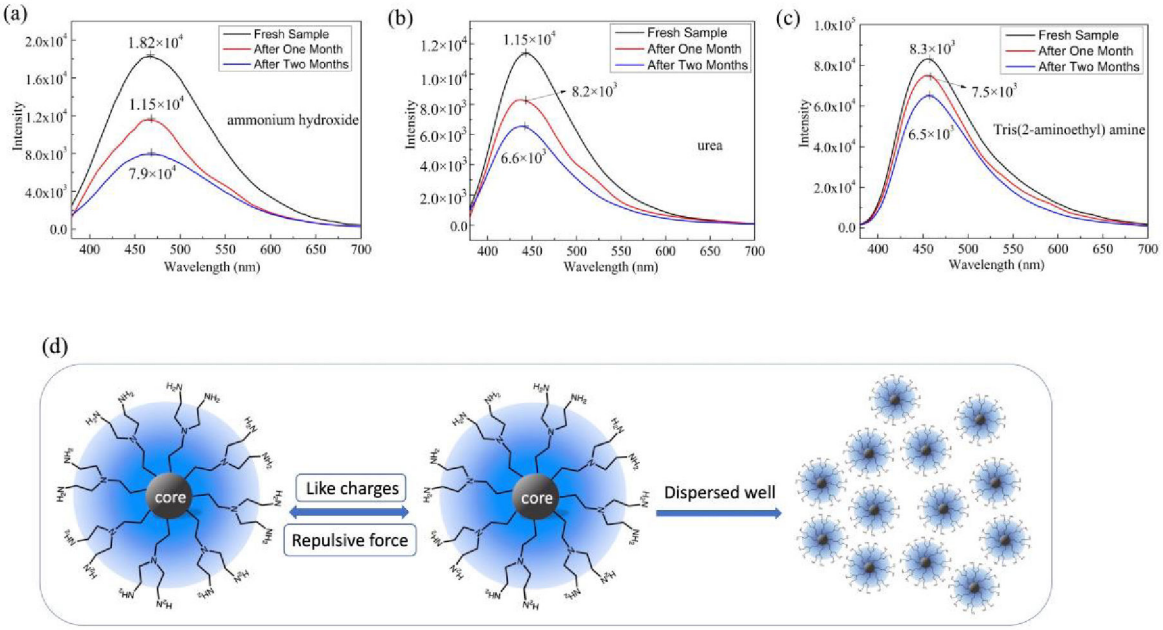

Figure 5.

Fluorescence intensity changes of CPDs aqueous solutions during storages of one and two months. The CPDs were prepared by using (a) ammonium hydroxide, (b) urea, (c)TAEA as the nitrogen sources, respectively. (d) The high dispersion property mechanism of CPDs

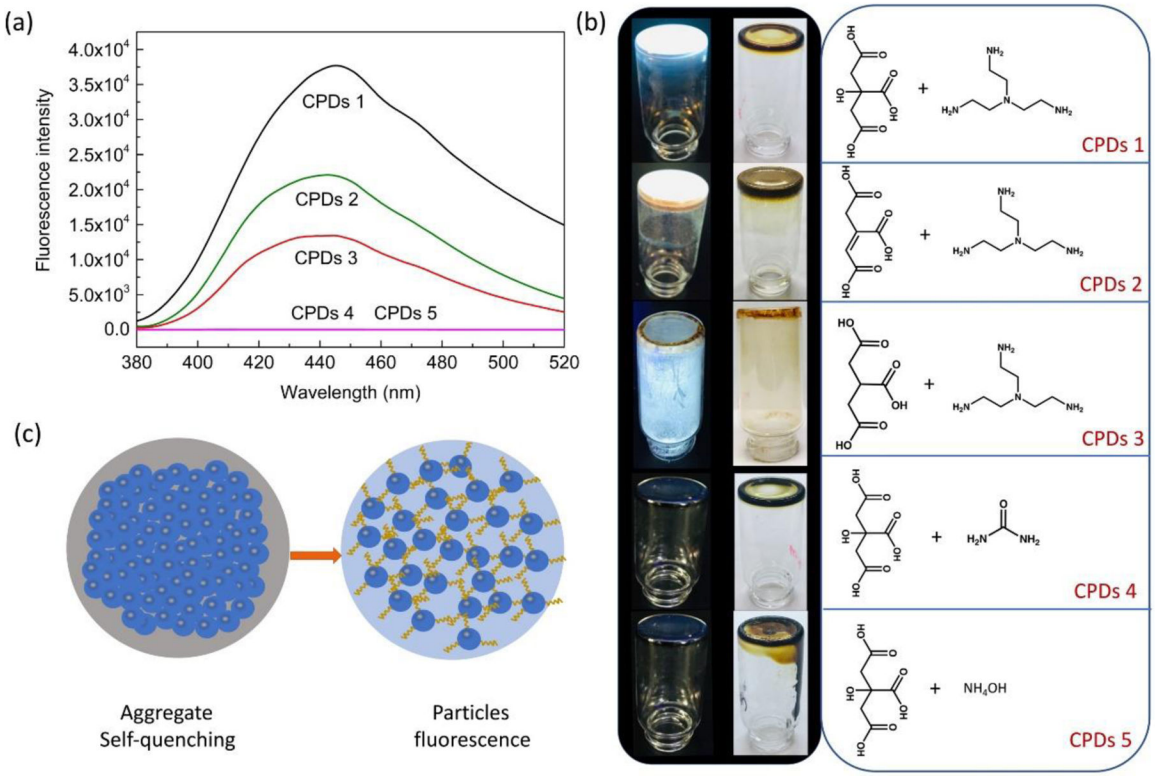

Figure 6.

(a) Fluorescence intensity changes of solid-state CPDs prepared by different starting materials. (b) The solid-state CPDs prepared by different starting materials under UV (left) and visible light (right). (c) The self-quenching mechanism of traditional CPDs and self-quenching-resistant mechanism of the core-shell dendritic structured CPDs.

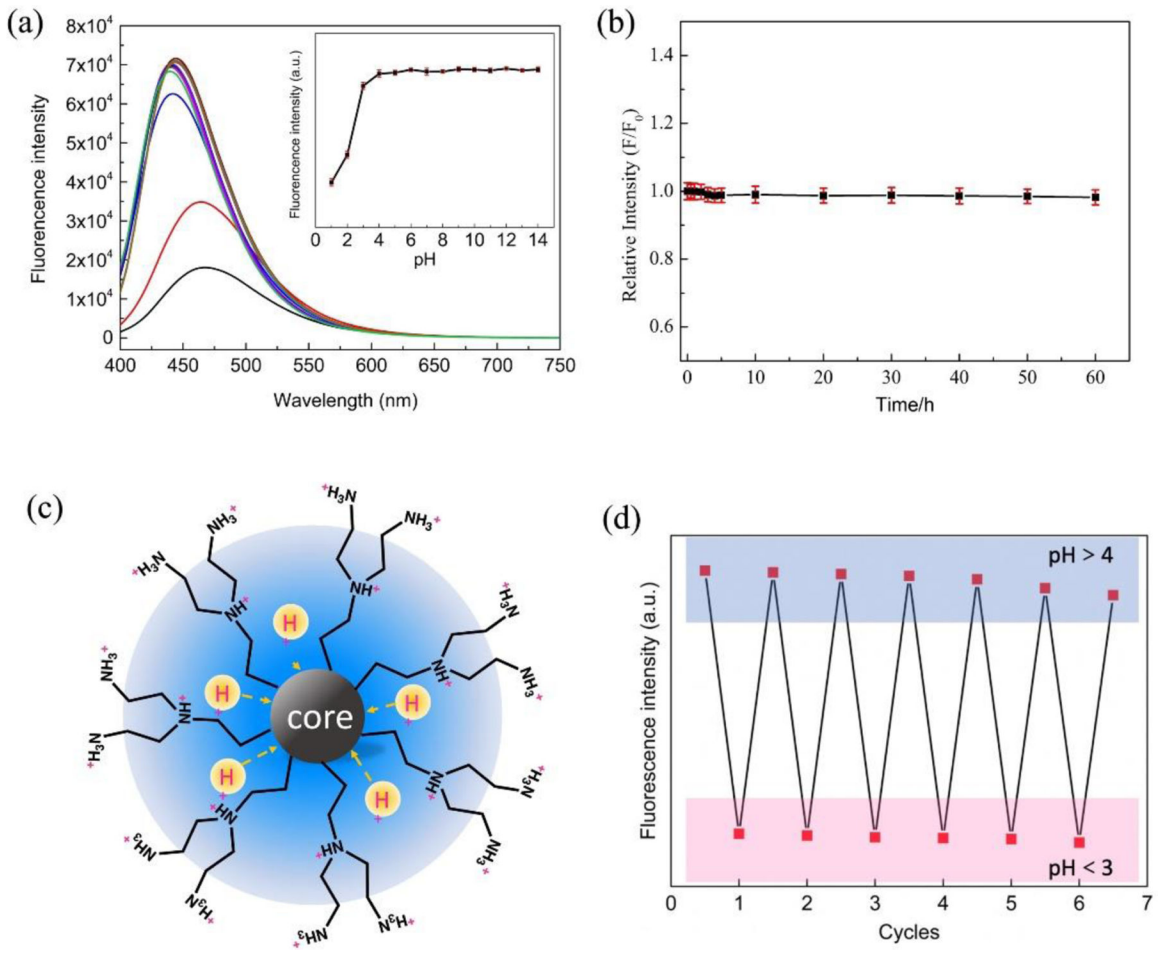

Figure 7.

(a) Fluorescence spectra of CPDs in solutions with different pH values (pH=1–14). (b) The fluorescence intensity of CPDs placed under UV light (365nm) during 0 to 60 hours. Data are presented as the average ± standard deviation (n=3). (c) The mechanism of fluorescence quenching (pH =1–3). (d) Fluorescence intensity changes of CPDs switching repeatedly under varied pH values from neutral to extremely acidic conditions and vice versa.

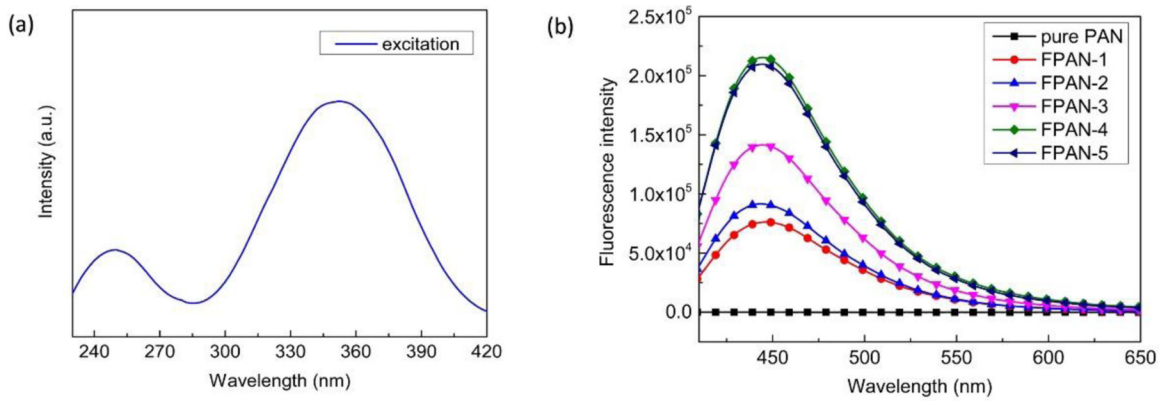

Figure 8.

Optical characterization of fluorescent PAN: (a) excitation spectra; (b) emission spectra with different fibers containing different concentrations of CPDs (CPD concentrations in FPAN-1, FPAN-2, FPAN-3, FPAN-4, and FPAN-5 were 0.01, 0.05, 0. 2, 0.5, and 1.0 wt.%, respectively)